ELSEVIER

Respiration Physiology 123 (2000) 153–164

RESPIRATION PHYSIOLOGY

www.elsevier.com/locate/resphysiol

A mathematical model of diffusion-limited gas bubble dynamics in tissue with varying diffusion region thickness

R. Srini Srinivasan [a,*], Wayne A. Gerth [b], Michael R. Powell [c]

[a] *Wyle Laboratories, 1290 Hercules Drive, Suite 120, Wyle Laboratories, Houston, TX 77058-2769, USA*
[b] *Navy Experimental Diving Unit, 321 Bullfinch Road, Panama City, FL 32407-7015, USA*
[c] *Environmental Physiology Laboratory, NASA Johnson Space Center, Houston, TX 77058-3691, USA*

Accepted 26 June 2000

Abstract

The three-region model of gas bubble dynamics consists of a bubble and a well-stirred tissue region with an intervening unperfused diffusion region previously assumed to have constant thickness and uniform gas diffusivity. As a result, the diffusion region gas content remains unchanged as its volume increases with bubble growth, causing dissolved gas in the region to violate Henry's law. Earlier work also neglected the relationship between the varying diffusion region volume and the fixed total tissue volume. The present work corrects these theoretical inconsistencies by postulating a difference in gas diffusivity between an infinitesimally thin layer at the bubble surface and the remainder of the diffusion region, thus allowing both thickness and gas content of the diffusion region to vary during bubble evolution. The corrected model can yield bubble lifetimes considerably longer than those yielded by earlier three-region models, and meets a need for theoretically consistent but relatively simple bubble dynamics models for use in studies of decompression sickness (DCS) in human subjects.

Keywords: Diffusion, gas bubble; Disease, decompression sickness; Gas, diffusion, bubble; Model, gas bubble

1. Introduction

Divers, aviators and astronauts risk occurrence of decompression sickness (DCS) when subjected to sufficiently rapid and extensive decreases in their ambient pressures. DCS is thought to arise from the formation and growth of gas bubbles in tissues, but the anatomic sites at which such formation occurs to cause DCS symptoms and signs are unknown. Thus, many of the pathophysiological processes of DCS can be theoretically described, but practical application of the theories requires specification of a number of tissue-specific biophysical parameters that remain unknown. Statistical methods are now being used to determine these parameters analytically from an ever-growing body of laboratory data (Gerth and Vann, 1996, 1997). These methods are very computation-intensive and the numbers of parameters

* Corresponding author. Tel.: +1-281-2121440; fax: +1-281-2121346.
E-mail address: srinivasan@klsiems.jsc.nasa.gov (R.S. Srinivasan).

0034-5687/00/$ - see front matter
PII: S0034-5687(00)00173-0

that can be determined are limited by the extent of available data. A model of bubble dynamics is required that is sufficiently general to accommodate in vivo conditions involved in DCS while remaining theoretically self-consistent, computationally simple, and parsimonious in the number of parameters it requires.

We recently examined candidate models for these purposes in some detail (Srinivasan et al., 1999). In 'two-region' models, the bubble is immersed in a uniformly perfused but unstirred tissue compartment; gas exchange between bubble and tissue is limited by bulk diffusion through the tissue. In 'three-region' models, the bubble is immersed in a well-stirred tissue compartment, and is immediately surrounded by a well-defined boundary layer through which diffusion-limited exchange of gas between bubble and tissue occurs. We showed that the dynamics of any one bubble cannot influence those of another in the two-region model. The three-region model, on the other hand, provides a description of bubble dynamics in a finite volume of tissue. Multiple bubbles in a compartment can thus be considered, with each competing for a finite amount of dissolved gas to limit the growth of other bubbles in the compartment and influence the kinetics of inert gas washout via the perfusate. The ability to model such cases is required to test formulations of DCS risk as functions of both the volume and profusion of in vivo bubbles (Gerth and Vann, 1995).

Although the three-region model developed earlier is computationally simple, it requires the radial gas flux to be the same everywhere in the diffusion region and assumes that the thickness of this region is constant. As a result, the gas content of the diffusion region remains unchanged while the volume of the region varies with bubble size and the gas tension in the region varies with ambient pressure and perfusion processes in the well-stirred region. This behavior violates Henry's law, which requires that the concentration of an inert gas in any liquid region vary in proportion to the gas tension. We herein extend the three-region model to eliminate this violation by allowing both the thickness and gas content of the diffusion region to vary during bubble evolution. The changes in diffusion region gas content are attributed to a difference in gas fluxes at the inner boundary of the diffusion region. The relationship between the flux difference and the rate of change of gas content in the diffusion region leads to a simple equation for calculating the diffusion region thickness. The present theoretical study is aimed at developing a consistent but relatively simple description of bubble dynamics for use in DCS studies, and does not consider any experimental data.

2. Model description

The model, schematized in Fig. 1, differs from previous three-region models (Gernhardt, 1991; Srinivasan et al., 1999) in how the diffusion region surrounding the bubble is defined. As before, this is an unstirred, unperfused region of finite thickness through which diffusion-limited gas exchange between bubble and tissue occurs. Unlike earlier models, however, the thickness of this region is allowed to vary without limit up to the entire tissue volume during bubble evolution. At the inner boundary of this region coinciding with the bubble surface, we identify a thin layer which may have a gas diffusivity less than that of the remainder of the region. A well-stirred region with uniform gas concentration and tension lies outside the diffusion region. Thus, strictly speaking, the model comprises four regions, but we simplify it to a three-region representation by neglecting the thickness of the bubble surface layer.

We consider all gases involved in bubble growth to be ideal. The equations developed below pertain to a single diffusible gas and exclude solvent vapor pressure. These equations can be readily generalized to accommodate solvent vapor pressure, other gases, and tissue elastic effects as described earlier (Srinivasan et al., 1999) and elaborated in Appendix A.

2.1. The diffusion equation

Neglecting convection due to bubble movement, gas diffusion through the region surrounding the bubble with no sources or sinks is described by the general diffusion equation:

$$\frac{\partial c}{\partial t} = D_b \nabla^2 c \quad (1)$$

where c is concentration of gas in tissue (in moles per unit volume), D_b is diffusivity of the gas in the diffusion region surrounding the bubble, and t is time.

We solve the diffusion equation by invoking the quasi-static approximation (Keller, 1964); i.e. by assuming $\partial c/\partial t = 0$. This is justified as long as the bubble equilibrates with its surrounding tissue much faster than changes in tissue gas concentration occur from perfusion effects or changes in ambient pressure or breathing gas. We then assume spherical symmetry, replace the partial derivatives by total derivatives, and expand the right side of Eq. (1) to obtain:

$$\frac{\partial^2 c}{\partial r^2} + \frac{2}{r}\frac{\partial c}{\partial r} = 0 \quad (2)$$

where r denotes the radial distance from the center of the bubble.

Present conceptualization of the bubble-tissue system suggests the following boundary conditions for solution of Eq. (2): $c(r_i, t) = \alpha_t P_i(t)$ and $c(r_o, t) = \alpha_t P_t(t)$, where r_i and r_o are the inner and outer radii of the diffusion region, respectively, with corresponding gas pressures P_i and P_t, and α_t is the tissue solubility (in moles per unit volume per unit pressure). The gas pressure P_t at the outer radius is equal to the uniform tissue gas tension in the well-stirred region. The gas pressure P_i at the inner radius is equal to the bubble gas pressure, assuming the thickness of the bubble surface to be negligible compared to that of the diffusion region. Neglecting the deformation pressure due to tissue elasticity, the gas bubble pressure is given by:

$$P_i = P_{amb} + \frac{2\sigma}{r_i} \quad (3)$$

where P_{amb} is ambient pressure and σ is surface tension.

The following expressions for the gas concentration and its gradient in the diffusion region ($r_i \le r \le r_o$) are obtained by integrating Eq. (2) twice and using the boundary conditions to evaluate the integration constants:

$$c(r, t) = \alpha_t P_t - \alpha_t (P_t - P_i)\frac{r_i}{h}\left[\frac{r_o}{r} - 1\right] \quad (4a)$$

and

$$\frac{dc}{dr} = \frac{\alpha_t (P_t - P_i)}{r^2}\frac{r_o r_i}{h} \quad (4b)$$

where $h = r_o - r_i$ is the thickness of the diffusion region. Eq. (4a) yields the following expression for

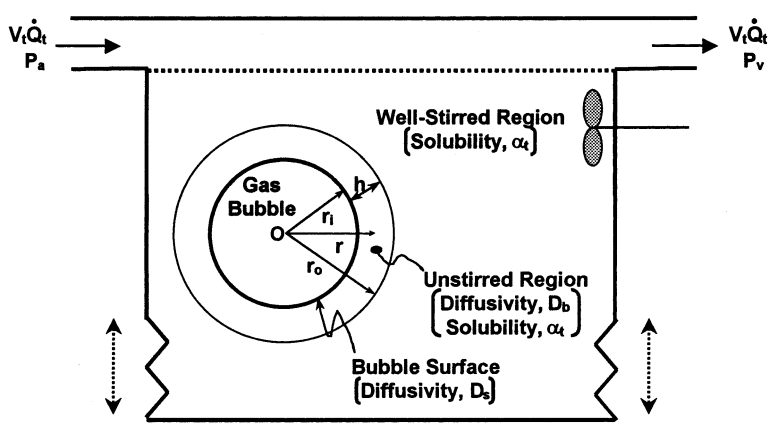

Fig. 1. Small-scale three-region model of a gas bubble. The bubble, with center at o, has a surface of negligible thickness with diffusivity D_s. Beyond this surface lies an unstirred diffusion region with no blood flow and a well-stirred region with uniform gas concentration. Dotted double-headed arrows indicate that the overall compartmental volume varies with r as the compartmental liquid volume V_t remains constant. The blood flow is $\dot{Q}_t$ per unit volume of the tissue and the total blood flow is $V_t\dot{Q}_t$. The symbols P_a and P_v denote the arterial and venous gas tensions, respectively.

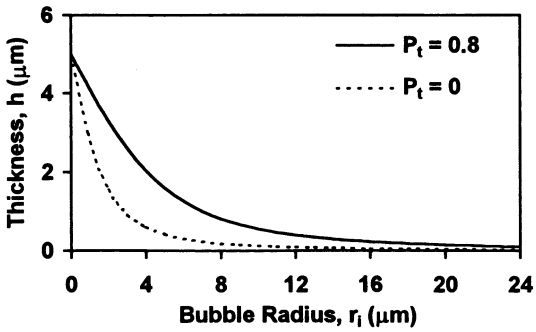

Fig. 2. Dependence of diffusion region thickness on bubble radius for fixed values of the parameters in Eq. (6). Assuming constant gas diffusivity throughout the diffusion region of a three-region bubble dynamics model, this equation prescribes the variations in diffusion region thickness required for dissolved gas to follow Henry's law in the diffusion region during bubble evolution. A lower tissue gas tension P_t in the well-stirred region results in faster bubble resolution, as would be expected. $P_{amb} = 5$ psia; $\sigma = 30$ dynes/cm.

the gas content of the diffusion region, U_d (in moles):

$$U_d = \int_{r_i}^{r_o} c(r, t) 4\pi\rho^2 d\rho = \alpha_t \left[P_t V_d - \frac{2\pi r_i h}{3} (3r_i + h)(P_t - P_i) \right] \quad (5)$$

where ρ is the dummy variable of integration with respect to radial distance, and $V_d = (4\pi/3)(r_o^3 - r_i^3)$ is the diffusion region volume.

2.2. Equations for diffusion region thickness

The gas flux at any radial distance r within the diffusion layer is given by the product of the diffusivity D_b, the concentration gradient dc/dr, and the surface area $4\pi r^2$ (Fick relationship). It follows from Eq. (4b) that the flux f_o across the outer boundary of the diffusion region at $r = r_o$ equals the flux f_i across the bubble surface at $r = r_i$. Because of this equality of fluxes, the gas content of the diffusion region remains unchanged during bubble evolution. With a constant h, as in our earlier three-region model (Srinivasan et al., 1999), such an unchanging gas content violates Henry's law. The violation can be avoided if the diffusion region thickness (and volume) is varied to produce changes in diffusion region gas concentration and tension appropriate to maintain a constant gas content. An expression for the required variation is obtained from Eq. (5) by expanding V_d in terms of r_i and h, and substituting P_i from Eq. (3). The resultant cubic equation in h, given below, is solved for h for any constant value of U_d:

$$(2P_t)h^3 + [(5P_t + P_{amb})r_i + 2\sigma]h^2 + 3r_i[(P_t + P_{amb})r_i + 2\sigma]h = (3/2\pi)\frac{U_d}{\alpha_t} \quad (6)$$

Note that the gas content of the diffusion region cannot be zero, because $h = 0$ is the only admissible solution to Eq. (6) with a zero value for U_d (the other two roots yield negative values for h).

Although gases in the diffusion region follow Henry's law under Eq. (6), the thickness h of the diffusion region rapidly diminishes as the bubble grows (Fig. 2). With constant gas diffusivity, the diffusion region offers decreasing diffusive resistance to gas flux into the bubble. As a result, gas tensions in the bubble and its surroundings rapidly approach equilibrium, and the dynamics of continued bubble growth are no longer diffusion-limited. Once the diffusion region is brought into theoretical conformance with Henry's law, bubble evolution can evidently remain diffusion limited only if the gas content of the diffusion region is allowed to vary. Given that the diffusion region is unperfused, such variation can occur only if the fluxes, f_o and f_i, are unequal. Requisite flux inequality is obtained if the diffusivity at the bubble surface D_s is different from the diffusivity D_b in the remainder of the diffusion region. We assume a higher resistance to diffusion at the bubble surface, and accordingly, D_s to be less than D_b. This is the simplest assumption leading to gas fluxes that are unequal but proportional (Eq. (7) below). Because the concentration gradient and the surface area are the same for both f_o and f_i at the bubble surface, we infer from the Fick relationship that:

$$\frac{f_i}{f_o} = \frac{D_s}{D_b} \quad (7)$$

Thus, a differential diffusivity in the diffusion region with constant values of D_s and D_b results

in proportionality of fluxes f_i and f_o. Using Eqs. (5) and (7) and expressing the flux f_i as the rate of change of bubble gas content, we obtain the following mass balance equation for the diffusion region:

$$\frac{dU_d}{dt} = \alpha_t \frac{d}{dt}\left[P_t V_d - \frac{2\pi r_i h}{3}(3r_i + h)(P_t - P_i) \right] = f_o - f_i = (\beta - 1)\frac{1}{RT}\frac{d(P_i V_i)}{dt} \quad (8)$$

where R is the gas constant, T is temperature, $V_i = (4\pi/3)r_i^3$ is bubble volume, and $\beta = D_b/D_s$ is the diffusivity ratio ($\beta > 1$ because $D_s < D_b$).

Eq. (8) is integrated to yield:

$$P_t V_d - \frac{2\pi r_i h}{3}(3r_i + h)(P_t - P_i) = k_d P_i V_i \quad (9)$$

where $k_d = (\beta - 1)/\alpha_t'$ and α_t' is the solubility expressed in units that include the factor RT. We have taken the constant of integration to be zero so that h vanishes along with r_i upon bubble resolution. Eq. (8) permits a zero value for the constant of integration so long as $\beta > 1$. In the degenerate case of $\beta = 1$, Eq. (8) reduces to $dU_d/dt = 0$, and U_d is a non-zero constant. This is consistent with Eq. (6) in which U_d cannot be zero, as noted earlier.

Following the same steps used to derive Eq. (6), we then obtain the following cubic equation in h:

$$(2P_t)h^3 + [(5P_t + P_{amb})r_i + 2\sigma]h^2 + 3r_i[(P_t + P_{amb})r_i + 2\sigma]h = (3/2\pi)k_d P_i V_i \quad (10)$$

Under Eq. (10), the diffusion region thickness is a function of the size and content of the gas bubble as well as the tissue gas tension.

2.3. Equation for rate of change of bubble radius

The equation for the rate of change of bubble radius is obtained from the rate of change of bubble gas content, which is given by the flux f_i. From Eq. (4b) and the Fick relationship, we obtain:

$$\frac{1}{RT}\frac{d(P_i V_i)}{dt} = 4\pi\alpha_t D_s (P_t - P_i)\frac{r_i r_o}{h} \quad (11)$$

which yields the following equation for dr_i/dt after substituting Eq. (3) for P_i on the left side, expanding the differential, and expressing V_i in terms of r_i:

$$\frac{dr_i}{dt} = \frac{\alpha_t' D_s (P_t - P_i)\left(\frac{1}{h} + \frac{1}{r_i}\right) - \frac{r_i}{3}\frac{dP_{amb}}{dt}}{P_{amb} + \frac{4\sigma}{3r_i}} \quad (12)$$

This rate equation is equivalent to that in our previous three-region model (Srinivasan et al., 1999) if $D_s = D_b$ and h is constant.

2.4. Gas tension in the well-stirred region

The equation for determining the uniform gas tension in the well-stirred region is derived by considering the mass balance for this region. Mass balance implies that the sum of gas fluxes and tissue gas contents in any given time interval must equal the amount of gas transported by perfusion. Thus, we have:

$$f_o + \frac{d}{dt}\int_{r_o}^{r_\infty} c(\rho, t)4\pi\rho^2 d\rho = \alpha_b \dot{Q}_t \int_{r_o}^{r_\infty} [P_a - P(\rho, t)]4\pi\rho^2 d\rho \quad (13)$$

where r_∞ is outer radius of the tissue, α_b is gas solubility in blood (in moles per unit volume per unit pressure), $\dot{Q}_t$ is blood flow per unit volume of well-stirred tissue, and P_a is arterial gas tension. Note that the outer tissue radius r_∞ is irrelevant to solution of either integral in Eq. (13), indicating that the tissue need not be spherical in shape.

The integral on the left side of Eq. (13) evaluates to $\alpha_t P_t(V_t - V_d)$ and the integral on the right side to $(P_a - P_t)(V_t - V_d)$, where V_t is the total volume of the tissue. Substituting the evaluated expressions for the integrals, relating f_o to f_i according to Eq. (7), expressing f_i as the rate of change of bubble gas content, dividing by $\alpha_t V_t$ throughout, and rearranging terms, Eq. (13) becomes:

$$\frac{d}{dt}[(1 - v)P_t] = (1 - v)\frac{P_a - P_t}{\tau} - \frac{\beta}{\alpha_t' V_t}\frac{d(P_i V_i)}{dt} \quad (14)$$

Table 1
Values of model parameters used in simulations. The diffusion region thickness parameter (h for the CT model and k_d for the VTDD model) was varied

Parameter	Value
Initial (critical) bubble radius	5 μm
Surface tension, σ	30 dynes/cm
Bubble surface diffusivity, D_a	1.32×10^{-6} cm^2/min
Tissue solubility, α'_t	0.0125 ml gas/ml tissue-atm
Tissue half-time, 0.693τ	60 min
Tissue volume, V_t (range)	$10^6 - 10^{10}$ μm^3

where $v = V_d/V_t$ is diffusion region fraction of the total tissue volume, and $\tau = \alpha_t/\alpha_b\dot{Q}_t$ is time constant of the tissue. When the diffusion region is a thin layer, $v \ll 1$ and Eq. (14) with $\beta = 1$ is the same as the simpler dP_t/dt expression for a three-region model of bubble dynamics used earlier (Srinivasan et al., 1999). For a large tissue, $V_t \rightarrow \infty$, $v \rightarrow 0$, and Eq. (14) further reduces to the familiar first-order equation in which the rate of change of tissue gas tension is proportional to the difference between arterial and tissue gas tensions. The solution of the more general Eq. (14) is involved because of the presence of the dv/dt term on the left side. Evaluation of dv/dt is obviated by solving Eq. (14) for P_t numerically using a method described in Appendix A.

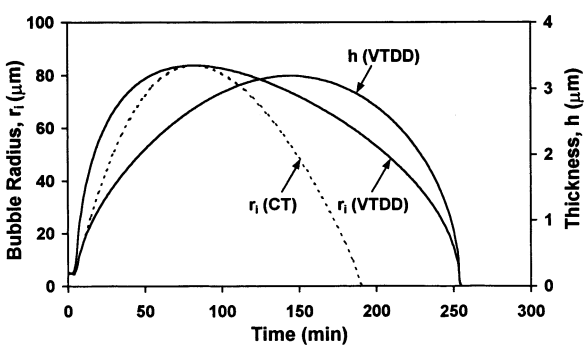

Fig. 3. Comparison of bubble radius profiles obtained with the VTDD ($k_d = 0.1$) and CT (h = 1 μm) models using the decompression described in the text, a tissue half-time of 60 min, and a tissue volume of 10^{10} μm^3. The peak radius (83 μm) and time to peak radius (82 min) are the same in both cases, but the VTDD model yields a higher bubble lifetime than the CT model (255 vs. 190 min). In the VTDD model, the diffusion region thickness increases as the bubble grows and continues to increase during the initial period of bubble resolution. After reaching a maximum thickness at ~140 min, the diffusion region contracts with continued diminution of the bubble to vanish with the bubble.

2.5. The complete model

Eqs. (3), (10), (12) and (14), with the expressions for V_i, V_d, and h, completely describe the dynamics of a gas bubble surrounded by a variable thickness, differential diffusivity (VTDD) diffusion region in a finite tissue. Model exercise requires simultaneous solution of two ordinary differential equations, one for the bubble radius and one for the tissue gas tension. The model parameters to be specified are σ, τ, α'_t, D_s, k_d, V_t, and the initial value of bubble radius r_i. The diffusion region thickness h is calculated from Eq. (10) for given values of tissue gas tension P_t, ambient pressure P_{amb}, bubble radius r_i, and parameters σ and k_d. The calculation can be completed analytically using Cardan's formula for cubic polynomials (Marcus and Minch, 1966), obviating the need for any iterative procedure.

3. Results

Bubble evolution after a decompression from sea-level to altitude was modeled using the VTDD model and a 'CT' model with a constant diffusion region thickness. The latter was the same as our previous three-region model (Srinivasan et al., 1999), except we here included the diffusion region volume (factor v in Eqs. (14) and (A3)) in the calculation of tissue gas tension P_t. The decompression profile consisted of ascent at 5000 ft/min to an indefinitely long residence at 30 000 ft breathing pure oxygen. Bubble growth began during ascent (decompression) from an assumed ever-present bubble nucleus of 5 μm radius upon attainment of the appropriate critical supersaturation given by Eq. (3). Other parameter values used are given in Table 1.

Fig. 3 shows the results obtained using values of k_d and h selected to yield the same peak radius during bubble evolution under either model in our sample profile. The time to peak radius is also the

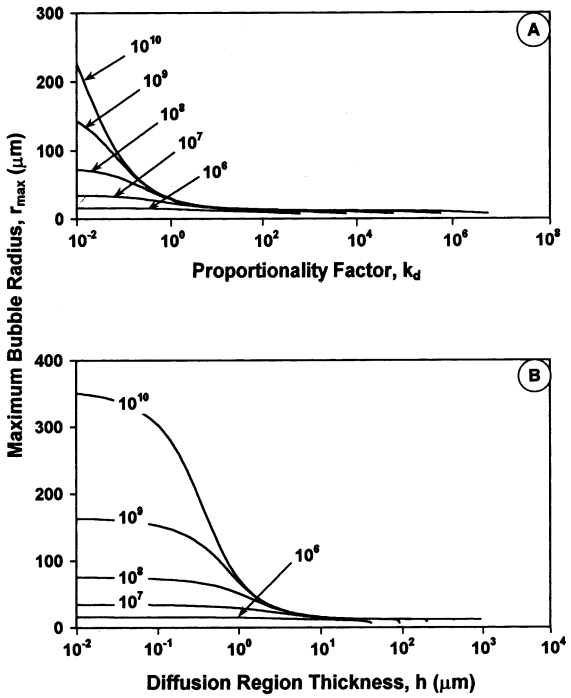

Fig. 4. Maximum bubble radius during the decompression described in the text as a function of k_d in the VTDD model (A) or h in the CT model (B) for tissue volumes ranging from 10^6 to 10^{10} μm^3 (indicated by arrows or labels). The upper limit of k_d and h is reached when the diffusion region occupies almost the entire tissue volume ($V_d \approx V_t$).

same for the two models under these conditions, but the VTDD bubble lifetime is approximately 33% longer than the CT bubble lifetime. Such bubble lifetimes can be obtained with the CT model only by increasing the tissue half-time. The longer bubble lifetime of the VTDD model arises from the increase in diffusion region thickness that accompanies bubble growth and continues through the initial period of subsequent bubble resolution. In the present example, the diffusion region thickness increases from bubble inception at the nucleonic size to reach a maximum ~ 60 min after the time of maximum bubble radius. Such a behavior contrasts with that obtained using the empirical function suggested by Tikuisis et al. (1982), in which r_i and h always vary in parallel. The greater thickness, and hence greater volume, of the diffusion region reduces the gas flux out of the bubble and allows the bubble to persist longer.

Fig. 4 shows how the dependence of the maximum bubble radius on k_d or h in the VTDD and CT models, respectively, varies with tissue volume from 10^6 to 10^{10} μm^3. The maximum bubble radius decreases with increasing k_d or h, but this decrease is more gradual with increasing k_d in the VTDD model than with increasing h in the CT model, especially at high tissue volumes. The latter model yields a large decrease in r_{max} as h is increased from 0.1 to 1 μm. Both models yield smaller r_{max} at lower tissue volumes as r_{max} becomes less sensitive to k_d or h.

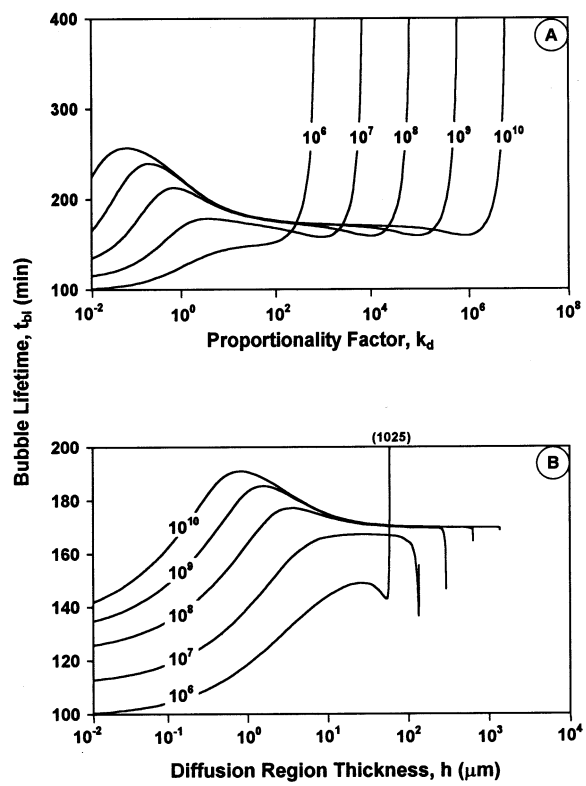

Fig. 5. Bubble lifetime as a function of k_d in the VTDD model (A) or h in the CT model (B) for the decompression described in the text and indicated tissue volumes ranging from 10^6 to 10^{10} μm^3. The upper limit of k_d and h is reached when the diffusion region occupies almost the entire tissue volume ($V_d \approx V_t$). The largest lifetime yielded by the CT model at $V_t = 10^6$ μm^3 is shown in parentheses at the top of panel B.

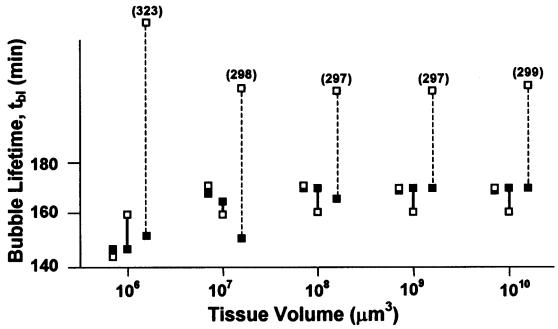

Fig. 6. Bubble lifetimes during the decompression described in the text produced by the VTDD (□) and CT (■) models at different tissue volumes for given maximum diffusion region volume to tissue volume fraction, v_{max}, during bubble growth. The three columns at each tissue volume correspond to v_{max} of 5% (left), 50% (middle), and 95% (right). The numbers in parentheses on top are lifetimes for the VTDD model at 95% v_{max}.

Fig. 5 shows the dependence of bubble lifetime t_{bl} on k_d or h in the two models. The curves are similar in shape except at large values of k_d or h, where the diffusion region volume approaches the total tissue volume ($v \rightarrow 1$). Each curve terminates with a respective k_d or h determined by v arbitrarily close to 1. The corresponding limiting value of k_d or h is thus the lowest value at which the diffusion region volume expands to equal the overall tissue volume during bubble growth. In the VTDD model (Fig. 5A), the bubble lifetime increases sharply and smoothly to asymptotically approach infinity as $v \rightarrow 1$ in a fashion that is consistent across the whole range of tissue volumes. In contrast, bubble lifetimes in the CT model (Fig. 5B) increase as $v \rightarrow 1$ only at low tissue volumes ($< 10^7$ μm^3). At high tissue volumes ($> 10^7$ μm^3), bubble lifetimes sharply decrease as $v \rightarrow 1$, so that the peak bubble lifetime for a given V_t occurs at a value of h lower than its limiting value at $v = 1$.

It is useful to compare bubble lifetimes prescribed by the two models for a fixed maximum $v = v_{max}$ (ratio of maximum diffusion region volume to tissue volume) during bubble growth. Fig. 6 shows the lifetimes produced by the models at different tissue volumes for three different values of v_{max} (5, 50 and 95%). Bubble lifetime at any v_{max} is nearly invariant with tissue volume in either model. However, the sensitivity of the VTDD bubble lifetime to high values of v is clearly evident. At any tissue volume, the VTDD and CT bubble lifetimes are almost the same at 5% v_{max}, but at 95% v_{max} the VTDD bubble lifetime is considerably larger than the CT bubble lifetime. It should be noted that such large lifetimes in the VTDD model are associated with large values of k_d that in turn correspond to diffusion region thicknesses far in excess of typical 10–20 μm intercapillary distances.

Both models responded similarly to changes in initial bubble radius and tissue half-time. Larger initial bubble sizes resulted in higher maximum bubble volumes, and larger tissue half-times resulted in prolonged bubble lifetimes.

4. Discussion

We showed previously that the three-region model is suitable for consideration of diffusion-limited dynamics of more than one bubble in a given tissue compartment (Srinivasan et al., 1999). Multiple bubbles in the model compete for finite amounts of dissolved gas in the well-stirred region, which limits the maximum bubble volumes attained during bubble growth and affects the kinetics of inert gas washout from the tissue. We have shown in present work that the constant gas diffusivity and diffusion region thickness assumed in this earlier work cause dissolved gas in the diffusion region to violate Henry's law. Moreover, the relationship between the diffusion region volume and the fixed total tissue volume was also neglected in this earlier work, because only cases in which the diffusion region volume is a small fraction of the overall tissue volume were considered. In present work, the CT model corrects the latter of these earlier theoretical inconsistencies, while the VTDD model corrects both.

The CT model was implemented for comparison to the VTDD model to illuminate how dissolved gas conformance to Henry's law in the diffusion region impacts three-region model behavior. The CT model is thus an extension of the earlier three-region model applicable to the dynamics of bubbles under conditions in which the

diffusion region volume constitutes a substantial fraction of the overall tissue volume. Such conditions occur at low tissue volumes or high bubble number densities. Like the VTDD model, the CT model accommodates effects of the varying fraction of overall tissue volume occupied by the diffusion region, under the constraint that $V_d \leq V_t$.

Dissolved gas fails to follow Henry's law in the diffusion region of both the earlier three-region model and the present CT model because the gas content of this region is forced to remain constant, while the volume of the region varies under the constraint of constant thickness. One remedy to this problem is to allow the gas content of the diffusion region to remain constant while varying the thickness of the region to keep its volume constant. However, this remedy results in a rapid decrease of diffusion resistance to tissue-bubble gas exchange during bubble growth and practical elimination of diffusion limitation to bubble growth.

An alternate solution to the problem is implemented in the VTDD model, which retains considerable diffusion limitation to bubble growth under most conditions. In this model, the dissolved gas content of the diffusion region varies in accord with Henry's law because of a postulated difference in gas diffusivity between the diffusion region and the bubble surface. As a result of this difference, and with no additional model constraints, variations of diffusion region thickness are theoretically prescribed in accord with the ratio of the diffusivities. Determination of these variations requires solution of a cubic polynomial, but the consequent increase in computational overhead is minimal. The model yields more regular and consistent behavior across physiological ranges of the parameters and can predict longer bubble lifetimes in compartments with shorter half-times than the other three-region models considered. The latter can be obtained because the diffusion region increases in thickness even as the bubble decreases in volume, and acts as a buffer zone that extends the bubble lifetime by retaining outwardly diffusing gas.

The consistency of the VTDD model is typified by the behavior illustrated in Fig. 5A. At given V_t, bubble lifetime varies smoothly with increasing k_d, passing through a maximum at an intermediate value of k_d at all but the lowest tissue volumes, and always asymptotically approaching infinity as k_d is increased toward its limiting value. Similar behavior is exhibited by the CT model only at very low tissue volumes ($< 10^7$ μm^3). Under such conditions, bubble lifetimes increase with high values of h as $v \rightarrow 1$, but the lifetimes are always smaller than those that can be achieved in a VTDD model with the same tissue volume and appropriately high k_d. At higher tissue volumes, bubble lifetime in the CT model can sharply decrease as h approaches its limiting value. As a result, the VTDD model can produce a wider range of bubble lifetimes than the CT model at any given tissue volume.

Both the VTDD and CT models include an implicit and interesting coupling of bubble evolution to overall compartmental blood flow, because the diffusion region volume changes with bubble radius in either model. Both assume the diffusion region to be devoid of blood flow and stipulate constant overall tissue volume. Changes in diffusion region volume are thus accompanied by changes in the remaining volume of well-stirred or perfused tissue. Overall blood flow to the tissue must consequently vary with r_i to maintain a constant compartmental time constant. In the limit where $v = 1$, and the entire tissue is in the diffusion region, blood flow to the tissue must be zero, and the bubble must remain indefinitely without resolving. Only the VTDD model properly simulates this phenomenon. Under steady ambient pressure the condition $v = 1$ occurs in both models at $r_i = r_{max}$ when $P_t = P_i$ and dr_i/dt is zero (Eq. (12)). Eq. (10) for the VTDD model then ensures that $dP_t/dt = 0$, so that P_t stays 'frozen' at P_i and the bubble remains at $r_i = r_{max}$. (Simultaneous solution of dP_t/dt and dh/dt using Eqs. (14) and (10) with k_d at its limiting value shows that dr_i/dt, dh/dt, and dP_t/dt all attain zero values at the instant v attains unity. The interval between the peak bubble radius and peak diffusion region thickness decreases with k_d, and vanishes when k_d reaches its limiting value.) In the CT model, on the other hand, dP_t/dt is undefined at the instant v attains unity (Eq. (14) is satisfied

for $v = 1$ with any dP_t/dt). Thus, the lifetime of a bubble in the CT model is finite at all tissue volumes and values of h, which is anomalous as h approaches and attains its upper limiting value.

At low values of k_d, the diffusivity of the diffusion region differs very little from the diffusivity of the bubble surface. The ratio of these diffusivities β is determined for given values of k_d and α'_tusing the formula for k_d shown below Eq. (9). With a solubility of 0.0125 ml/ml atm, the value for nitrogen solubility in water at 37°C used in our simulations, D_b exceeds D_s by little more than one percent for $k_d = 0.1$ used to generate the data in Fig. 3. The sensitivity of model behavior to such small differences in diffusivities underscores the importance of the present identification of the bubble surface as distinct from the diffusion region. We include the bubble surface here as the negligibly thin inner boundary of the diffusion region. It is possible to account for the distinctive properties of this boundary in a separate, finite thickness bubble surface region, which would expand the present model into a four-region model. Such a four-region model would provide a more realistic transition of gas flux from f_o to f_i with changes in diffusivity and gas concentration gradient through the thin bubble surface layer. However, little would be gained by such a model elaboration, because gas flux at any inter-regional boundary must be discontinuous as long as the problem is formulated in terms of distinct radial regions. For example, the present model already incorporates an abrupt change in gas flux from zero in the well-stirred region to a finite value just inside the diffusion region (at $r = r_o$). The abrupt transition from f_o to f_i at the bubble surface is simply an adoption of how a more gradual change behaves in the limit as the surface layer thickness approaches zero.

Arbitrarily long bubble lifetimes can be produced using the VTDD model, but only with large values of k_d and concomitant large values of the diffusion region thickness. For example, at the lowest tissue volume of 10^6 μm^3, the diffusion region thickness of ~ 54 μm obtained in our simulation at the limiting value of k_d is greater than typical 10–20 μm intercapillary distances. At higher V_t, the high values of k_d required for sustaining the bubble over longer times correspond to even higher diffusion region thicknesses. Physiologically consistent accommodation of such large diffusion region volumes requires relaxation of the present assumption of zero blood flow in the diffusion region. An extension of the VTDD model that includes blood flow in the diffusion region while remaining consistent with the present formulation is currently under development.

Acknowledgements

This work was supported in part by NASA Cooperative Agreement NCC 9-42 and US Navy contract N0463A-97-M-0126 (to WAG).

Appendix A

A.1. Generalization of the VTDD model

Model Eqs. (3), (12) and (14) of the VTDD model can be readily extended to include solvent vapor pressure, other gases, and tissue elastic effects using methods described in our previous article (Srinivasan et al., 1999). According to Eq. (10), however, the thickness h of the diffusion region must be calculated separately for each diffusible gas using its own tissue gas tension and partial pressure in the bubble. As a result, the diffusion region thickness is different for the different diffusible gases involved. This holds even if the same k_d is assumed for the gases, which would implicitly and unrealistically require that the diffusivity ratio D_b/D_s be the same for all gases. The VTDD model requirement of a different diffusion region thickness profile for each diffusible gas illustrates that the diffusion region is only a fictitious layer around the bubble into which all diffusion limitation to bubble dynamics is theoretically assigned. The assignment is made for mathematical convenience, not to imply that the region corresponds precisely to any actual physical layer.

A.2. Numerical solution of Eq. (14)

Eq. (14) is numerically solved for P_t by ignoring the (small) change in v at each integration step, i.e. by treating v(t) as a constant in each integration interval. Dividing by $(1-v)$ and rearranging terms, Eq. (14) becomes:

$$\frac{dP_t}{dt}+\frac{P_t}{t}=\frac{P_a}{t}-\frac{\beta}{\alpha_t V_t(1-v)}\frac{dX}{dt} \quad (A1)$$

where X denotes the product P_iV_i. Eq. (A1) holds with v(t) as a constant in each integration interval $[t,\ t+\Delta t]$, where Δt is the integration step size. Multiplying both sides of Eq. (A1) by $e^{t/\tau}$, and integrating between t and $t+\Delta t$, we obtain:

$$\begin{aligned}&P_t(t+\Delta t)e^{(t+\Delta t)/\tau}-P_t(t)e^{t/\tau}\\&=P_a(t)[e^{(t+\Delta t)/\tau}-e^{t/\tau}]\\&\quad+\dot{P}_a[(\Delta t)e^{(t+\Delta t)/\tau}-\tau e^{(t+\Delta t)/\tau}+\tau e^{t/\tau}]\\&\quad-\frac{\beta}{\alpha_t' V_t[1-v(t)]}\int_t^{t+\Delta t}e^{s/\tau}\left.\frac{dX}{dt}\right|_{t=s}ds\end{aligned} \quad (A2)$$

where s is the dummy variable of integration with respect to time, and $\dot{P}_a$ is the rate of change in arterial gas tension.

The integral in Eq. (A2) is evaluated by approximating X(t) by a straight line in each integration interval, so that

$$\left.\frac{dX}{dt}\right|_{t=s}=\frac{X(t+\Delta t)-X(t)}{\Delta t} \quad \text{for } t\le s\le t+\Delta t$$

Evaluating the integral and rearranging terms, we get the following expression for tissue tension at $(t+\Delta t)$ from Eq. (A2):

$$\begin{aligned}P_t(t+\Delta t)&=P_t(t)+\dot{P}_a\Delta t\\&\quad+\left[P_a-\dot{P}_a\tau-P_t(t)\right.\\&\quad\left.-\frac{\beta\tau}{\Delta t}\frac{[X(t+\Delta t)-X(t)]}{\alpha_t' V_t[1-v(t)]}\right](1-e^{-\Delta t/\tau})\end{aligned} \quad (A3)$$

Note that as $V_t\to\infty$, the last term within brackets on the right side of Eq. (A3) becomes zero, and the solution reduces to the expression for P_t in a bubble-free tissue. Also, with a diffusion region volume small compared to total tissue volume and equal gas fluxes under steady ambient conditions, $v=0$, $\beta=1$, and $\dot{P}_a=0$; Eq. (A3) then reduces to our earlier Eq. (B9) in Srinivasan, et al. (1999).

Bubble evolution is tracked by first solving Eqs. (10) and (12) for h and r_i, respectively, assuming P_t to be constant in the interval $[t,\ t+\Delta t]$, in accord with the quasi-static approximation. P_t is then updated for the next integration step using Eq. (A3). Consequently, Eq. (A3) is used only once during each integration step. Moreover, the exponential factor $(1-e^{-\Delta t/\tau})$ needs to be evaluated only once for each combination of Δt and τ values.

Appendix B. Nomenclature

atm	atmospheres (1 atm = 1013 kPa = 1.013×10^6 dynes/cm^2)
α_b	solubility of gas in blood (moles per unit volume per unit pressure)
α_t	tissue gas solubility (moles per unit volume per unit pressure)
α_t'	tissue gas solubility in practical units (ml gas/ml tissue-atm)
β	diffusivity ratio at bubble surface, D_b/D_s (dimensionless)
ρ	dummy variable of integration with respect to radial distance (μm)
σ	surface tension (dynes/cm)
τ	tissue time constant associated with tissue blood flow (min)
A_i	surface area of bubble (μm^2)
D_b	diffusion region diffusivity (cm^2/min)
D_s	diffusivity of gas at bubble surface (cm^2/min)
h	diffusion region thickness (μm)
f_i	gas flux at bubble surface (moles/min)
f_o	gas flux at outer boundary of diffusion region (moles/min)
k_d	proportionality factor associated with variable diffusion region thickness (dimensionless)
P(r, t)	tissue gas tension in diffusion region (atm)
P_a	arterial gas tension (atm)
$\dot{P}_a$	rate of change in arterial gas tension (atm/min)

P_{amb}	ambient pressure (atm)
P_i	gas pressure in bubble (atm)
P_t	tissue gas tension in the well-stirred region (atm)
P_v	venous gas tension (atm)
$\dot{Q}_t$	blood flow per unit volume of tissue (min^{-1})
r	radial distance from the center of bubble (μm)
r_i	inner radius of diffusion region (μm)
r_o	outer radius of diffusion region (μm)
r_∞	outer radius of tissue (μm)
s	dummy variable of integration with respect to time (min)
t	time (min)
t_{bl}	bubble lifetime (min)
V_i	bubble volume (μm^3)
V_d	diffusion region volume (μm^3)
V_t	tissue volume (μm^3)
v	diffusion region volume fraction, V_d/V_t (dimensionless)
v_{max}	maximum value of v (dimensionless)
U_d	diffusion region gas content (moles)
X	product, P_iV_i (atm-μm^3)

References

Gernhardt, M.L., 1991. Development and evaluation of a decompression stress index based on tissue bubble dynamics. PhD Dissertation, University of Pennsylvania.

Gerth, W.A., Vann, R.D., 1995. Statistical bubble dynamics algorithms for assessment of altitude decompression sickness incidence. USAF Armstrong Laboratory Technical Report, AL/CF-TR-1995-0037, Brooks AFB, Texas.

Gerth, W.A., Vann, R.D., 1996. Development of iso-DCS risk air and nitrox decompression tables using statistical bubble dynamics models. Final Report Contract no. NA46RU0505, National Oceanic and Atmospheric Administration, Office of Undersea Research, Bethesda, MD.

Gerth, W.A., Vann, R.D., 1997. Probabilistic gas and bubble dynamics models of DCS occurrence in air and N_2O_2 diving. Undersea Hyper. Med. 24 (4), 275–292.

Keller, J.B, 1964. Growth and decay of gas bubbles in liquids. In: Davies, R. (Ed.), Proceedings Symposium on Cavitation in Real Liquids. Elsevier, New York, pp. 20–29.

Marcus, M., Minch, H., 1966. Modern University Algebra. MacMillan Company, New York, pp. 200–201.

Srinivasan, R.S., Gerth, W.A., Powell, M.R., 1999. Mathematical models of diffusion-limited gas bubble dynamics in tissue. J. Appl. Physiol. 86, 732–741.

Tikuisis, P., Ward, C.A., Venter, R.D., 1982. Bubble evolution in a stirred volume of liquid closed to mass transport. J. Appl. Physiol. 54, 1–9.